PHYSICAL REVIEW C VOLUME 24, NUMBER 5 NOVEMBER 1981

Configuration space Faddeev calculations. V. Variational bounds

J. L. Friar and B. F. Gibson
Theoretical Division, Los Alamos National Laboratory, Los Alamos, New Mexico 87545

G. L. Payne
Los Alamos National Laboratory, Los Alamos, New Mexico 87545
and Department of Physics and Astronomy, University of Iowa, Iowa City, Iowa 52242
(Received 11 May 1981)

Three three-nucleon model problems are proposed as test cases for numerical computation: the ground and excited states of a spin-isospin independent Yukawa potential (Delves potential) and the ground state of a spin-isospin independent potential composed of one attractive and one repulsive Yukawa function (Malfliet-Tjon V). Eigenvalues and eigenfunctions are calculated using a configuration space Faddeev approach, and variational upper and lower bounds are evaluated using these wave functions. Each calculation is performed both as a projected s-wave potential problem, and as a true local potential problem in which nucleon-nucleon partial waves through $l=6$ are kept. For each case the eigenvalue appears to be converged to within 1 keV and it agrees well with the upper bound. A brief review of bounding techniques is presented.

[NUCLEAR STRUCTURE Variational bounds, three-body problem.]

I. INTRODUCTION

Many techniques have been used to solve the Schrödinger equation for the three-nucleon system. The earliest technique used was the variational method.[1] Thomas[2] in 1935 used this method to demonstrate that zero-range forces lead to a collapse of the ground state. During the decade beginning in 1960, the variational technique was the primary method of calculating properties of the trinucleon system.[3] Many different procedures exist for developing the trial functions used in these calculations. Some resort to intuition[4] in order to build in such features as the wave function suppression caused by strongly repulsive potential components. Others rely on systematic, brute force expansions, typified by the use of a harmonic oscillator basis set.[5,6] Another more recent development is the hypernetted chain expansion.[7]

Alternatively, one may use the Schrödinger equation in different forms. A direct attempt has been made to solve the Schrödinger equation; this was only moderately successful.[8] A second approach, the hyperspherical expansion of the Schrödinger equation, approximates the original equation by a truncated series of coupled differential equations in a single (hyperspherical) radius variable.[9] A more recent technique, applied to the four-nucleon problem and nuclear matter, is the Green's function Monte Carlo method,[10] which also has its variational counterpart. The decade beginning in 1970 has been dominated by the Faddeev method,[11] which replaces the Schrödinger equation with a different equation (or set of coupled equations) and solves the new equation. The latter technique exists in both configuration space[12,13] and momentum space[14] versions, and as a mixture of both.[15]

All of these methods "work" for the *bound* states in the sense that the boundary conditions (finiteness, and vanishingly small wave functions at infinity) are implementable to arbitrary accuracy in principle, and are tractable in practice. It remains to be seen which technique is best in practice, that is, a solution achieved to a given level of accuracy with the least effort. Recently, a study[16] of the features of the wave functions of various model problems has shown that for simple smooth potentials with no repulsion, the wave functions are largely featureless, and presumably every method works reasonably well. In contradistinction with this conclusion, the wave functions for models with strong short range repulsion show considerable structure. A strong argument was made in such

cases that the Faddeev method is easier to implement numerically than the variational method, because much of the structure is produced when the "smooth" Faddeev amplitude ψ_1 is permuted to form the complete Schrödinger wave function $\Psi \equiv \psi_1 + \psi_2 + \psi_3$. That is, the permuted functions ψ_2 and ψ_3, which are obtained "free" in the Faddeev approach, build in rapid variations in Ψ which are not present in ψ_1.

Nevertheless, the complexity associated with solving a (set of) differential equation(s) in three independent coordinate variables is formidable, and there has been considerable controversy over the accuracy of various calculations. This problem has been compounded by an important practical consideration: some methods, including the Faddeev one, perform a partial wave decomposition of the nucleon-nucleon force and keep only a finite set of these waves, while other methods, including the variational, traditionally keep all partial waves. Thus, the problems which are solved are not the same, and different answers are to be expected. To the best of our knowledge, there exists no set of semirealistic model problems (or even one) which has been used as a test of the various techniques. Only the widely used but esthetically unpleasing separable potentials are available, as well as the unphysical harmonic oscillator problem. In the latter problem, interestingly enough, the Faddeev solution is far more complex than the Schrödinger one.[17]

In this work, we propose a set of three problems; each involves a local potential but without the complexity of a tensor component or spin-isospin dependence. These "homework" problems (in Bethe's original sense) are not new, but we feel they provide a reasonable test of calculational methods, and are therefore a useful check for old and new techniques. This is our primary motivation, since we feel that the lack of homework problems has been an impediment to the field. The problems discussed here all involve a sum of Yukawa functions for the nucleon-nucleon potential in the form

$$V(r) = \left[-V_A e^{-\mu_A r} + V_R e^{-\mu_R r} \right] / r \ , \qquad (1)$$

where V_A and V_R are both positive. Each of these "boson" problems, so called because they do not involve spin in any way, has characteristic difficulties associated with achieving a solution. The first model problem involves the ground state of the Delves potential,[18] with $V_R \equiv 0$, which is deeply bound and structureless. The second problem involves the (only) excited state of the same model, which necessarily has more structure. The third problem involves the ground state of the Malfliet-Tjon V (MT-V) potential,[19] which has strong repulsion.

Two basic criteria exist for the "goodness" of a solution: the accuracy of the energy eigenvalue, and variational upper and lower bounds. Clearly, the first criterion requires a known solution of verifiable accuracy. The second criterion is sometimes used to provide such a verification, and, indeed, is the only mechanism which exists for purely variational calculations to estimate eigenvalues. We will combine these two criteria.

Our approach will be as follows for each of the problems. Using a partial wave decomposed potential, the nonrelativistic configuration space Faddeev-Noyes equation[20] for a Hamiltonian H will be solved for a sufficient number of partial waves to generate an eigenvalue converged to within 1 keV. For each of the partial wave cases, the wave functions we obtain will be used to calculate $\langle H \rangle$ and $\langle H^2 \rangle^{1/2}$ (where the potential used in H is the complete potential), whence variational upper and lower bounds can be obtained for the complete (all partial waves) problem. Variational bounds for the case of a purely s-wave potential will also be calculated.

In addition to providing a good illustration of the use of variational bounds, which are briefly reviewed in Sec. II, this approach also illustrates the rate of convergence of the partial wave expansion. To the best of our knowledge, this is the first Faddeev calculation which has been forced to numerical "completion." The use of variational bounds also provides us with a lower bound on the overlap of the "exact" wave function with the numerically calculated one, and thus a further check on the quality of the wave function, as well as the associated eigenvalue. We will see that the higher partial waves in Ψ which are induced by the permuted coordinates in ψ_2 and ψ_3 provide good variational estimates for the effect of the higher partial waves in the potential, even when ψ_1 is calculated using s-waves *only*. The purely s-wave potential version of the homework problems is a good check for Faddeev codes which treat only s-wave interactions. Calculational and numerical method details will be provided in Sec. III and the Appendix, while tables of convergence of eigenvalues, upper and lower bounds, and values of $\langle H \rangle$ and $\langle H^2 \rangle^{1/2}$ will be given in Sec. IV.

II. VARIATIONAL BOUNDS

Variational principles are older than quantum theory, and were implemented at a very early stage in the development of quantum mechanics.[1,21] The best known of these is the Rayleigh-Ritz variational principle, which states that the lowest eigenvalue E_0 of the Hamiltonian H satisfies the inequality

$$E_0 \leq \langle 0 | H | 0 \rangle \ , \tag{2a}$$

where $|0\rangle$ is *any* well-behaved, normalized (to one) trial function; the equality holds if $|0\rangle \equiv |\psi_0\rangle$, the lowest eigenfunction of H. The relationship clearly does not hold for excited states $E_1, E_2, \ldots$, since the ground state trial function $|0\rangle$ used in place of the excited state trial function $|i\rangle$ produces an obvious contradiction. One way around this is to diagonalize H simultaneously for the first N states, producing orthogonal trial functions, which then satisfy[22]

$$E_k \leq \langle k | H | k \rangle, \quad k \leq N \ . \tag{2b}$$

This procedure works very well, since it is well known[1] that an error of magnitude ϵ in $|0\rangle$ [i.e., $(|\psi_0\rangle - |0\rangle) \sim \epsilon$] produces an upper bound higher than E_0 by a magnitude proportional to ϵ^2.

Although the true eigenvalue lies below the Ritz upper bound, it is difficult to know by how much. This is the utility of lower bounds, although in practice lower bounds often work poorly, and wave functions which produce good upper bounds can produce poor lower bounds. Four lower bound techniques are commonly used and are the simplest: (1) The august Temple bound,[23] predating quantum mechanics; (2) the Stevenson[24] bound; (3) the Weinstein bound[25]; and (4) the Hall-Post bound.[26] The first three are improvable, in the sense that better wave functions yield better (higher) lower bounds, while the Hall-Post bound is fixed for a given problem. Other bounding techniques are discussed in the excellent presentation of Hill[27] and in the review by Weinhold.[28]

We always assume that we are dealing with normalized wave functions. We define

$$\bar{E}_k = \langle k | H | k \rangle < 0 \tag{3a}$$

and

$$\Delta_k = \langle k | H^2 | k \rangle^{1/2} + \bar{E}_k > 0 \ , \tag{3b}$$

where it is assumed[3] that one uses trial functions which satisfy $\langle k | H^2 | k \rangle \equiv \langle kH | Hk \rangle$. The latter form will always be used. The various improvable lower bounds satisfy $E_k \geq E_k^L$ and the various E_k^L are

Weinstein:

$$E_k^W = \bar{E}_k - (\Delta_k{}^2 - 2\bar{E}_k \Delta_k)^{1/2} \ , \tag{4a}$$

if

$$\bar{E}_k \leq \frac{(E_k + E_{k+1})}{2} \ ; \tag{4b}$$

Temple:

$$E_k^T = \frac{\alpha_T \bar{E}_k - (\bar{E}_k - \Delta_k)^2}{\alpha_T - \bar{E}_k} \ , \tag{5a}$$

if

$$\bar{E}_k < \alpha_T < E_{k+1} \ ; \tag{5b}$$

Stevenson:

$$E_k^S = \alpha_S - (\alpha_S^2 - 2\alpha_S \bar{E}_k + (\bar{E}_k - \Delta_k)^2)^{1/2} \ , \tag{6a}$$

if

$$\alpha_S \leq (E_k + E_{k+1})/2 \ . \tag{6b}$$

Thus, two of the bounds involve parameters. The best result for the Temple bound is achieved by choosing α_T as far from $\bar{E}_k$ as possible (i.e., $|\alpha_T|$ as small as possible or as close to E_{k+1} as possible), while the Stevenson result is best for α_S as close to $(E_k + E_{k+1})/2$ as possible (i.e., $|\alpha_S - \bar{E}_k|$ as small as possible). Note that choosing $\alpha_S = \bar{E}_k$ in the Stevenson formula produces the Weinstein result, which clearly will be inferior if the wave functions are good.

The major problem with implementing the Stevenson and Temple bounds lies in choosing the free parameters,[29] α, since both depend implicitly on the eigenvalues they are bounding. It can be shown that[30] given *only* E_{k+1}, Δ_k, and $\bar{E}_k$, the Temple bound is the best possible lower bound; however, it does involve an unknown: E_{k+1}. Given information on E_k also, the Stevenson bound may be better, as noted by Walmsely,[31] although Schmid and Schwager[30] have pointed out that given E_k, the best lower bound is, of course, E_k. If our only information is $\bar{E}_k$, $\bar{E}_{k+1}$, and Δ_k, Δ_{k+1} then the choices of α must be determined by this information. We are forced to use the lower bounds themselves in determining the α's and choose

$$\alpha_T = E_{k+1}^T \ , \tag{6c}$$

and

$$\alpha_S=(E^S_{k+1}+E^S_k)/2\ ; \tag{6d}$$

we therefore achieve a functional relationship for E^S_k which can be solved to yield a result for E^S_k which is identical to Eq. (5a) with $\alpha_T=E^T_{k+1}$. Thus, *the Temple and Stevenson bound are functionally identical.*[32] If $\Delta_k/\bar{E}_k$ is small (the result of using good trial wave functions), one then finds to first order in Δ_k,

$$E^S_k\cong\bar{E}_k+\frac{2\bar{E}_k\Delta_k}{E^S_{k+1}-\bar{E}_k} \tag{7a}$$

and

$$E^W_k\cong\bar{E}_k-(-2\Delta_k\bar{E}_k)^{1/2}\ , \tag{7b}$$

which clearly illustrates the superiority of the Stevenson (Temple) results. Note that the difference of the upper and lower bounds, $-E^S_k+\bar{E}_k$, has a "lever arm" of $2\bar{E}_k/(-E^S_{k+1}+\bar{E}_k)$. For a system with a *single* bound state, we know that $E^S_1\equiv 0$, and the Temple and Stevenson result is particularly simple:

$$E^L_0=\frac{\langle 0\,|\,H^2\,|\,0\rangle}{\langle 0\,|\,H\,|\,0\rangle}\cong\bar{E}_0-2\Delta_0\ . \tag{8}$$

Clearly, we wish Δ_0 to be as small as possible. The lever arm is smallest ($\equiv 2.0$) for a single bound state, and is somewhat larger in all other cases. For two bound states $E^S_2\equiv 0$; the result for E^L_1 consequently has the same form as Eq. (8) with $0\rightarrow 1$.

The upper bound when there is a single excited state can be handled in essentially two different ways. One of these uses a variation of the Stevenson bound,[5] while the other diagonalizes in the subspace of the ground and excited states; we will follow the latter procedure.

Another physically interesting bound is the Eckart bound,[21,25] which states that the overlap between a trial wave function Φ and the exact ground state wave function Ψ is bounded by

$$1\geq|\langle\Phi\,|\,\Psi\rangle|^2\equiv S^2\geq\frac{E_1-\langle\Phi\,|\,H\,|\,\Phi\rangle}{E_1-E_0}\ . \tag{9}$$

In any application we can replace E_1-E_0 in the denominator by the difference of upper and lower bounds, $E^U_1-E^L_0$, and replace E_1 in the numerator by E^L_1. If there is no excited state, $E_1\equiv 0$ and then

$$S\geq\frac{|\langle\Phi\,|\,H\,|\,\Phi\rangle|}{|\langle\Phi\,|\,H^2\,|\,\Phi\rangle|^{1/2}}\cong 1+\Delta_0/2\bar{E}_0\ . \tag{10}$$

Thus, $\Delta_0/\bar{E}_0$ provides a direct measure of the goodness of a trial wave function.

Finally, Hall and Post[26] have developed a nonimprovable lower bound for ground states, which uses an effective two-body Hamiltonian

$$H_{\rm eff}=\frac{p^2}{M}+\frac{3}{2}V(r)\ . \tag{11}$$

The bound is obtained by taking twice the lowest eigenvalue of $H_{\rm eff}$, which uses the usual two-body center-of-mass kinetic energy, and 1.5 times the two-body potential $V(r)$.

III. BOUND STATE WAVE FUNCTIONS

The wave functions used in the evaluation of the matrix elements of H and H^2 are calculated by the numerical solution of the Faddeev equations in configuration space. For three identical particles with coordinates $\vec{r}_1$, $\vec{r}_2$, and $\vec{r}_3$ we use the Jacobian coordinates[13]

$$\vec{x}_i=\vec{r}_j-\vec{r}_k\ , \tag{12a}$$

and

$$\vec{y}_i=\tfrac{1}{2}(\vec{r}_j+\vec{r}_k)-\vec{r}_i\ , \tag{12b}$$

where i, j, and k imply cyclic permutation. One set of these variables is shown in Fig. 1. The Hamiltonian for local potentials has the form

$$H=T+V(x_1)+V(x_2)+V(x_3)\ , \tag{13}$$

where T is the kinetic energy operator in the center-of-mass coordinates. The total wave function Ψ for the three-particle system is written as the sum of three terms

$$\begin{aligned}\psi&=\psi(\vec{x}_1,\vec{y}_1)+\psi(\vec{x}_2,\vec{y}_2)+\psi(\vec{x}_3,\vec{y}_3)\\&\equiv\psi_1+\psi_2+\psi_3\ .\end{aligned} \tag{14}$$

The Schrödinger equation can be separated into the three coupled equations

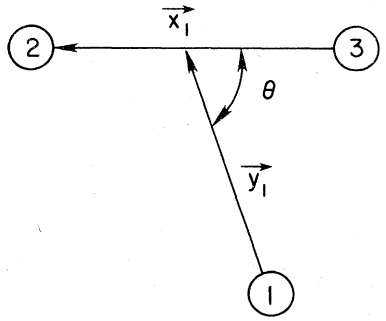

FIG. 1. The Jacobian coordinates for three particles.

$$[T+V(x_i)-E]\psi_i=-V(x_i)[\psi_j+\psi_k] \ . \tag{15}$$

Since the particles are identical the functions ψ_i all have the same functional form and it is only necessary to solve one of the three equations.

The total angular momentum of the system is zero; hence, the Faddeev amplitude ψ_1 can be written in the form

$$\psi(\vec{x}_1,\vec{y}_1)=\sum_l \frac{\phi_l(x_1,y_1)}{x_1y_1} \times\frac{(2l+1)^{1/2}}{4\pi}P_l(\mu_1) \ , \tag{16}$$

where $P_l(\mu_1)$ is the Legendre function and μ_1 is the cosine of the angle between $\vec{x}_1$ and $\vec{y}_1$. Using the symmetry of the ψ_i one obtains the following coupled equations for the reduced wave function $\phi_l(x_1,y_1)$:

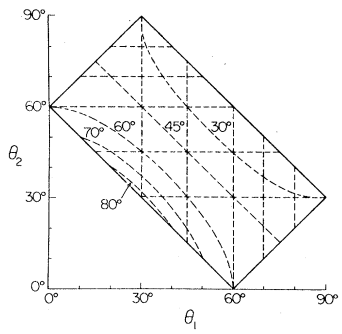

FIG. 2. The limits of the θ_2 integral in Eq. (21) are indicated by solid lines. Typical discontinuities in the integrand are illustrated by dashed lines. These discontinuities correspond to having knots in the θ_1, θ_2, and θ_3 variables at 0°, 30°, 45°, 60°, 70°, 80°, and 90°.

$$\left[\frac{\partial^2}{\partial x_1^{\,2}}+\frac{3}{4}\frac{\partial^2}{\partial y_1^{\,2}}-\frac{l(l+1)}{x_1^{\,2}}-\frac{3}{4}\frac{l(l+1)}{y_1^{\,2}}-U(x_1)-K^2\right]\phi_l(x_1,y_1)$$
$$=U(x_1)\int_{-1}^{1}d\mu_1\left[\frac{x_1y_1}{x_2y_2}\right]\sum_{l'}[(2l+1)(2l'+1)]^{1/2}P_l(\mu_1)P_{l'}(\mu_2)\phi_{l'}(x_2,y_2) \ , \tag{17}$$

where $K^2=-mE/\hbar^2$, $U(x_1)=mV(x_1)/\hbar^2$, and m is the mass of one particle. The permuted variables x_2 and y_2 are given by

$$x_2=\tfrac{1}{2}(x_1^{\,2}-4x_1y_1\mu_1+4y_1^{\,2})^{1/2} \tag{18a}$$

and

$$y_2=\tfrac{1}{2}(9x_1^{\,2}/4+3x_1y_1\mu_1+y_1^{\,2})^{1/2} . \tag{18b}$$

The value of μ_2, the cosine of the angle between $\vec{x}_2$ and $\vec{y}_2$, can be found from the relationship

$$x_1^{\,2}=\frac{1}{4}x_2^{\,2}+x_2y_2\mu_2+y_2^{\,2} \ . \tag{19}$$

For the actual numerical calculations it is more convenient[12,13] to use the variables ρ and θ_i defined by

$$x_i=\rho\cos\theta_i \tag{20a}$$

and

$$y_i=\frac{\sqrt{3}}{2}\rho\sin\theta_i \ . \tag{20b}$$

In terms of these variables the Faddeev equation has the form

$$\left[\frac{\partial^2}{\partial\rho^2}+\frac{1}{\rho}\frac{\partial}{\partial\rho}+\frac{1}{\rho^2}\frac{\partial^2}{\partial\theta_1^2}-\frac{4l(l+1)}{\rho^2\sin^2 2\theta_1}-U(\rho\cos\theta_1)-K^2\right]\phi_l(\rho,\theta_1)$$
$$=\frac{4}{\sqrt{3}}U(\rho\cos\theta_1)\sum_{l'}\int_{\theta_1^-}^{\theta_1^+}[(2l+1)(2l'+1)]^{1/2}P_l(\mu_1)P_l'(\mu_2)\phi_l'(\rho,\theta_2)d\theta_2 \ , \tag{21}$$

where the limits θ_1^- and θ_1^+ of the θ_2 integral are the solid lines shown in Fig. 2. The values of μ_1 and μ_2 are given by

$$\mu_1 = -\frac{1}{\sqrt{3}} \frac{\cos 2\theta_1 + 2\cos 2\theta_2}{\sin 2\theta_1} \tag{22a}$$

and

$$\mu_2 = \frac{1}{\sqrt{3}} \frac{\cos 2\theta_2 + 2\cos 2\theta_1}{\sin 2\theta_2} \ . \tag{22b}$$

To solve Eq. (21) we write each $\Phi_l(\rho,\theta_1)$ in the form

$$\Phi_l(\rho,\theta_1) = \rho F(\rho,\theta_1) e^{-K\rho} \ , \tag{23}$$

and expand $F(\rho,\theta_1)$ in a complete set of basis states. We choose as our basis set the bicubic splines on a rectangular grid in the $\rho-\theta_1$ coordinates,

$$F(\rho,\theta_1) = \sum_{m=1}^{M} \sum_{n=1}^{N} a_{mn} s_m(\rho) s_n(\theta_1) \ , \tag{24}$$

where the number of basis states is $M \times N$. The coefficients a_{mn} are determined by the method of orthogonal collocation.[13] For $s_m(\rho)$ and $s_n(\theta_1)$ we use the piecewise Hermite polynomials; these functions have continuous first derivatives, but the second derivatives are discontinuous at the knots. Consequently, when evaluating integrals of these functions the region of integration must be subdivided into a sum of regions defined by the knots. This point is discussed further in the Appendix.

The boundary conditions for $F(\rho,\theta_1)$ are

$$F(\rho,0) = F(\rho,\pi/2) = 0 \tag{25a}$$

and

$$F(\rho_{\max},\theta_1) = 0 \ , \tag{25b}$$

where $\rho_{\max}$ is the maximum value of the variable ρ. The boundary condition at $\rho = \rho_{\max}$ introduces obvious error into the wave function, but this error should "heal" within a short distance. If $\rho_{\max}$ is chosen to be sufficiently large, the error in the wave function will be negligible. The final test for the wave function is the difference between the upper and lower bounds on the energy calculated using that wave function.

IV. RESULTS AND DISCUSSION

For our calculations we used the parametrizations of Refs. 33 and 34. This was done in order to correspond as closely as possible to previous work. With the Delves potential we used $\hbar^2/m = 41.468$ MeV fm^2 and with the MT-V potential we used 41.470 MeV fm^2. The potential parameters used in the calculations are listed in Table I.

We first calculated eigenfunctions and eigenvalues for up to (and including) four channels; that is $l = 0,2,4,6$. For identical particles only even partial waves are allowed. A single s-wave ($l = 0$ only) calculation using a large number of basis states was made, as well as a series of calculations using a smaller number of basis states for each of the various l's but with exactly the *same mesh parameters* (i.e., the same knots and collocation points). The angular momentum barrier greatly reduces the effect of the higher partial waves, as can be seen in Table II. The topmost results are for the ground state of the Delves potential, and we list $\langle H \rangle$, $\langle H^2 \rangle^{1/2}$, the upper and lower bounds, E_U, E_L, the eigenvalue resulting from the Faddeev calculation, and the rms radius. For the Delves excited state results which are listed in the middle of the table, we have assumed, and will later justify in Table III, that $\langle 1 \mid H \mid 1 \rangle$ by itself gives the upper bound to E_1 correct to the indicated number of significant figures. The results for the MT-V potential are listed at the bottom of the table. The last significant figure listed in these tables is not necessarily accurate and this will be discussed later.

In Table II the column labeled "s wave" denotes the results obtained using wave functions from an s-wave Faddeev calculation, in which the variational part has also been performed assuming a po-

TABLE I. Parameters for Delves and MT-V potentials, as used in the calculations. Note that the MT-V potential that we use is the one given in Ref. 34, not the one in Ref. 19.

	V_R (MeV fm)	V_A (MeV fm)	μ_R(fm^{-1})	μ_A (fm^{-1})
Delves	0	49.7616·1.58	0	1/1.58
MT-V	1438.4812	570.3316	3.11	1.55

TABLE II. Expectation values, upper and lower bounds, Faddeev eigenvalues, and rms radii various potential models and for varying numbers of potential partial waves (channels). The energies are in MeV and radii in fm.

		s-wave	one channel	two channel	three channel	four channel
	$-\langle H\rangle$	50.5100	50.8271	50.8596	50.8600	50.8600
	$\langle H^2\rangle^{1/2}$	50.5100	51.0424	50.8686	50.8622	50.8615
Delves	$-E_U$	50.5100	50.8271	50.8596	50.8600	50.8600
	$-E_L$	50.5101	51.3558	50.8816	50.8655	50.8636
	$-E_F$	50.5093	50.5100	50.8419	50.8575	50.8595
	$\langle r^2\rangle^{1/2}$	0.802	0.8025	0.8026	0.8027	0.8027
	$-\langle H\rangle$	8.652	8.861	8.878	8.878	8.878
	$\langle H^2\rangle^{1/2}$	8.655	9.096	8.957	8.951	8.950
	$-E_U$	8.652	8.861	8.878	8.878	8.878
Delves*	$-E_L$	8.658	9.338	9.036	9.024	9.022
(excited state)	$-E_F$	8.652	8.660	8.864	8.883	8.886
	$\langle r^2\rangle^{1/2}$	2.69	2.697	2.649	2.647	2.647
	$-\langle H\rangle$	7.540	7.722	7.736	7.736	7.736
	$\langle H^2\rangle^{1/2}$	7.550	8.453	7.899	7.864	7.861
MT-V	$-E_U$	7.540	7.722	7.736	7.736	7.736
	$-E_L$	7.560	9.253	8.065	7.994	7.988
	$-E_F$	7.540	7.539	7.714	7.733	7.735
	$\langle r^2\rangle^{1/2}$	1.727	1.727	1.711	1.710	1.710

tential which acts only in s waves; this result is meant primarily to be a test for Faddeev codes. The Delves model ground state energy is well determined by the variational bounds, the upper and lower bounds differing by 0.17 keV. The Faddeev eigenvalue is above the lower bound by 0.7 keV, which is within the roughly 1 keV uncertainty in the eigenvalue. Because the Faddeev calculation is not variational, the Faddeev eigenvalue does not necessarily lie within these bounds. Since the magnitude of $\Delta_0/\bar{E}_0$ in Eq. (10) is approximately 10^{-6}, the overlap between the calculated and exact wave functions is virtually one. The n-channel results in the next few columns indicate the progression towards numerical completion of the full (all partial waves) problem, calculated using a smaller basis/channel than the first column. The D-wave contribution adds roughly 300 keV to the eigenvalue, while improving the upper bound by only 30 keV. The reason for this relatively small improvement in the bound compared to 300 keV is the induced D-wave components (coming from coordinate permutations in ψ_2 and ψ_3) in the Faddeev wave function calculated with s-wave potentials. In this respect the Faddeev wave functions calculated using s-wave potentials are "better" than the eigenvalue, as seen by comparing $\langle 0|H|0\rangle$ to the complete potential problem. Higher partial waves add little to the upper bound, while the lower bound improves considerably, an expected result. The radius increases very slightly as the binding increases. This is due to a cancellation between two opposing physical effects. The increased binding as higher partial waves are included shrinks the system, thereby decreasing the radius. In contradistinction, the higher partial waves are pushed out by the centrifugal barrier, thereby increasing the radius. For the nonrepulsive Delves interaction in the ground state, the centrifugal barrier effect is the more important.

The results for the Delves excited state are not as well converged as for the ground state. The s-wave eigenvalue lies very close to the upper bound, while the lower bound is 7.2 keV lower. The complete problem has an eigenvalue roughly 8 keV below the upper bound, which is itself 144 keV above the lower bound. The radius of the excited state *decreases* as the higher partial waves are included (increasing the binding), an indication that the nodal structure in the excited state wave function has pushed it out so that there is less of a difference between the $l=0$ and $l=2,4,\ldots$, com-

ponents.

The MT-V case is the least well converged, a reflection of the strong repulsion in the potential for small nucleon separations which requires a larger basis set to obtain the same level of accuracy. The upper bound for the s-wave problem is in good agreement with the eigenvalue and lies 20 keV above the lower bound. The eigenvalue for the complete problem lies about 1 keV above the upper bound, which is 252 keV above the lower bound. The radius decreases with the addition of higher partial waves (increasing the binding).

These numbers reflect a few simple phenomena which are relevant to all these cases.

(1) The s-wave functions yield quite good upper bounds to the complete problem because of the induced higher angular momentum components from the permuted parts of the wave function.

(2) The upper bounds are better converged than are the lower bounds.

(3) The Faddeev eigenvalues agree well with the upper bounds, but are considerably higher than the lower bounds.

(4) Less than 1 keV of binding can be expected from $l \geq 8$ waves, and convergence of the eigenvalue as a function of l is fairly rapid.

(5) The radii tend to decrease with increasing l (binding), except for very compact systems with nonrepulsive forces. The overall change is small, less than 2% in all cases.

(6) Any structure in the wave function, whether due to excited state nodes or repulsion in the potential can cause the lower bound to differ substantially from the upper bound.

We also note that the wave functions which give good upper bounds do not necessarily generate good lower bounds. We made little effort to find the mesh parameter sets which produced the best lower bounds, except for the s-wave case. In most cases the upper bounds were very similar, and finding better lower bounds did not change our belief that the eigenvalues and the upper bounds were virtually identical.

For comparison, we have also generated the Hall-Post (HP) lower bounds for the ground states. We find

$$E_L^{\mathrm{HP}} = -58.6 \text{ MeV} \quad \text{(Delves)}$$

and

$$E_L^{\mathrm{HP}} = -10.7 \text{ MeV} \quad \text{(MT-V)} \ .$$

They are not particularly useful when one has good trial wave functions, as we do.

The expected accuracy of the ground state eigenvalues is roughly 1 keV for the Delves case and 2 keV for the MT-V case while that of the excited state is perhaps 3 keV for the s-wave problem and 10 keV for the various entries in the complete problem. Estimating the accuracy of the Faddeev eigenvalue is a very subjective business, at best. None of the variational bounds would suggest, however, that our criteria for making these estimates are too restrictive. The accuracy of the quadratures involved in $\langle H \rangle$ and $\langle H^2 \rangle$ is somewhat easier to assess. The expectation values of the various pieces of H and H^2 were separately calculated on a Vax. It was found that double precision was essential because of enormous cancellations involving large numbers. The integration over each of

TABLE III. Upper bounds separated into components. The notations 0 and 1 refer to ground and excited states. All energies are in units of MeV, while the wave function overlaps are dimensionless.

	Delves		MT-V	
	s-wave	Complete	s-wave	Complete
$\langle 0 \mid V \mid 0 \rangle$	− 175.606	− 176.632	− 36.551	− 37.505
$\langle 0 \mid T \mid 0 \rangle$	125.096	125.772	29.011	29.768
$\langle 0 \mid H \mid 0 \rangle$	− 50.510	− 50.860	− 7.540	− 7.736
$\langle 1 \mid V \mid 1 \rangle$	− 43.947	− 45.392		
$\langle 1 \mid T \mid 1 \rangle$	35.295	36.514		
$\langle 1 \mid H \mid 1 \rangle$	− 8.652	− 8.878		
$\langle 0 \mid H \mid 1 \rangle$	0.000 25	− 0.0038		
$\langle 0 \mid 1 \rangle$	$-3.05 \cdot 10^{-6}$	8.03×10^{-5}		

the various regions determined by the knots of the splines was done by n-point Gauss quadrature. The upper bound was converged at the 0.01 keV level with four-point rules, while $\langle H^2\rangle^{1/2}$ required six-point rules. Even then, the difference between the six- and four-point results for the latter case was a few hundredths of a keV for the Delves cases, and a few tenths of a keV for the MT-V case. It is expected in each case that the error in the $\langle H^2\rangle^{1/2}$ quadratures is no more than 1 keV in the final result. (Note the tiny off-diagonal matrix elements in Table III.)

Using a standard variational approach Bell and Delves[3,33] calculated upper and lower bounds for their second (complete) potential ($\lambda=1.2$) and found -50.858 and -50.89 MeV, respectively. For the excited state, they found -8.87 and -10.83 MeV, respectively. Their upper bounds agree well with ours, while the difference between their upper and lower bounds is roughly a factor of 10 more than the difference between our bounds. For the s-wave MT-V problem Afnan and Reid[34] found a binding energy of 7.539 MeV, a number in good agreement with our upper bound and Faddeev eigenvalue.

In summary, we have calculated Faddeev eigenvalues and wave functions for a set of model homework problems. These wave functions were used to calculate variational upper and lower bounds using the Temple prescription; the former are consistent with the eigenvalues. The eigenvalues of the complete potential problem appears converged (to within 1 keV), using four partial waves.

Note added in proof It has come to our attention that some groups are working with a version of the MT-V potential inferred from Ref. 19 whose strength parameters differ from those listed in Table I: $V_A=578.089$ MeV fm and $V_R=1458.047$ MeV fm. Although this version of the MT-V potential does not yield the two-body binding energy quoted in Ref. 19, we give here the corresponding three-body results for completeness. The Faddeev eigenvalues, upper bounds, and lower bounds are denoted below in each case by $[-E_F, -E_U, -E_L]$ MeV. For the large basis calculation of the s-wave interaction (as the partial-wave local potential was *originally* defined) we find [8.0424, 8.0425, 8.0609], while the 2, 3, and 4 channel calculation results for the complete, local potential problem are given by [8.228, 8.252, 8.562], [8.249, 8.253, 8.490], [8.251, 8.253, 8.484]. The Faddeev eigenvalue in the last case lies 1.5 keV above the upper bound, whereas in the s-wave case it is 0.12 keV higher.

ACKNOWLEDGMENTS

This work was performed under the auspices of the U. S. Department of Energy. We would also like to acknowledge our debt to Patsy Rivera and Q Division of Los Alamos National Laboratory for their support of our computational effort.

APPENDIX

To evaluate the bounds for the energy one needs to evaluate the matrix elements of H and H^2. Using the symmetries of the total wave function these matrix elements can be expressed in terms of a few integrals. The form we used was found to be the most convenient. For example, the expectation value of H can be written as

$$\langle\Psi|H|\Psi\rangle=\langle\Psi|T|\Psi\rangle+\langle\Psi|V|\Psi\rangle\ , \quad \text{(A1)}$$

where

$$V=V(x_1)+V(x_2)+V(x_3)\equiv V_1+V_2+V_3\ .$$

Using Eq. (14) of Sec. III one can show that

$$\begin{aligned}\langle\Psi|V|\Psi\rangle&=3\langle\Psi|V_1|\Psi\rangle\\&=3[\langle\psi_1|V_1|\psi_1+2\psi_2\rangle\\&\quad+2\langle\psi_2|V_1|\psi_1+\psi_2+\psi_3\rangle]\ ,\end{aligned} \quad \text{(A2)}$$

and that

$$\langle\Psi|T|\Psi\rangle=3\langle\psi_1|T|\psi_1+2\psi_2\rangle\ . \quad \text{(A3)}$$

In a similar manner one writes

$$\langle\Psi|H^2|\Psi\rangle=\langle\Psi|(T^2+2TV+V^2)|\Psi\rangle\ , \quad \text{(A4)}$$

and the three terms in this expression can be written in the form

$$\langle\Psi|T^2|\Psi\rangle=3\langle T\psi_1|T\psi_1+2T\psi_2\rangle\ , \quad \text{(A5)}$$

$$\begin{aligned}\langle\Psi|TV|\Psi\rangle&=3[\langle T\psi_1|V_1|\psi_1+2\psi_2\rangle\\&\quad+2\langle T\psi_2|V_1|\psi_1+\psi_2+\psi_3\rangle]\ ,\end{aligned} \quad \text{(A6)}$$

and

$$\begin{aligned}\langle\Psi|V^2|\Psi\rangle&=3\langle\Psi|V_1{}^2|\Psi\rangle\\&\quad+6\langle\Psi|V_1V_2|\Psi\rangle\ ,\end{aligned} \quad \text{(A7)}$$

where

$$\begin{aligned}\langle\Psi|V_1{}^2|\Psi\rangle&=\langle\psi_1|V_1{}^2|\psi_1+2\psi_2\rangle\\&\quad+2\langle\psi_1|V_1{}^2|\psi_1+\psi_2+\psi_3\rangle\ ,\end{aligned} \quad \text{(A8)}$$

and

$$\langle\Psi|V_1V_2|\Psi\rangle = 2\langle\psi_1|V_1V_2|\psi_1+\psi_2+2\psi_3\rangle + \langle\psi_3|V_1V_2|\psi_3\rangle \ . \quad \text{(A9)}$$

The normalization integral can be written as

$$\langle\Psi|\Psi\rangle = 3\langle\psi_1|\psi_1+2\psi_2\rangle \ . \quad \text{(A10)}$$

For the actual numerical evaluation of the matrix elements it is convenient to use the variables ρ, θ_1, and θ_2. Therefore, we use the transformation

$$\int_0^\infty dx_1 \int_0^\infty dy_1 \int_{-1}^{1} d\mu_1 \left[\frac{x_1y_1}{x_2y_2}\right] \rightarrow 2\int_0^\infty \rho\, d\rho \int_0^{\pi/2} d\theta_1 \int_{\theta_1^-}^{\theta_1^+} d\theta_2 \ , \quad \text{(A11)}$$

where limits of the θ_2 integral are the solid lines in Fig. 2. Next the region of integration is subdivided into a sum of regions in which the integrand is well behaved, that is, where the various quantities in the integrand are continuous. Recall that the second derivatives of the Hermite polynomials are discontinuous at the knots.

From Fig. 2 one can see that the derivative of θ_1^- is discontinuous at $\theta_1=60°$ and that the derivative of θ_1^+ is discontinuous at $\theta_1=30°$. Therefore, the θ_1 integral is divided into an integral from 0° to 30°, an integral from 30° to 60°, and an integral from 60° to 90°. Each of these regions is further subdivided into regions where Ψ is well behaved; these regions are defined by the knots of ρ, θ_1, θ_2, and θ_3. The regions defined by the knots of ρ, θ_1, and θ_2 are readily identified since these are the variables of integration. The location of the knots of θ_3 in the θ_1-θ_2 plane are found from the relation

$$\cos2\theta_1 + \cos2\theta_2 + \cos2\theta_3 = 0 \ . \quad \text{(A12)}$$

An example of the division of the θ_1-θ_2 plane is shown in Fig. 2. The integration over each region was performed by Gaussian quadratures.

[1] F. L. Pilar, *Elementary Quantum Chemistry* (McGraw-Hill, New York, 1968) contains an excellent introductory treatment with many historical references.
[2] L. H. Thomas, Phys. Rev. 47, 903 (1935).
[3] L. M. Delves, Adv. Nucl. Phys. 5, 1 (1972) thoroughly reviews this aspect of the variational problem.
[4] M. A. Hennell and L. M. Delves, Nucl. Phys. A246, 490 (1975).
[5] G. L. Payne and L. Schlessinger, J. Comput. Phys. 13, 266 (1973).
[6] P. Nunberg, D. Prosperi, and E. Pace, Nucl. Phys. A285, 58 (1977).
[7] J. Lomnitz-Adler and V. R. Pandhari-Pande, Nucl. Phys. A342, 404 (1980).
[8] I. M. Bassett, B. R. E. Lederer, and G. C. Vorlicek, Phys. Lett. 51B, 329 (1974); J. Comput. Phys. 22, 34 (1976).
[9] J. L. Ballot and M. Fabre de la Ripelle, Ann. Phys. (N. Y.) 127, 62 (1980).
[10] J. G. Zabolitzky and M. H. Kalos, Nucl. Phys. A356, 114 (1981).
[11] Y. E. Kim and A. Tubis, Annu. Rev. Nucl. Sci. 24, 69 (1974) and A. C. Phillips, Rep. Prog. Phys. 40, 905 (1977) review this problem.
[12] A. Laverne and C. Gignoux, Nucl. Phys. A203, 597 (1973).
[13] G. L. Payne, J. L. Friar, B. F. Gibson, and I. R. Afnan, Phys. Rev. C 22, 823 (1980); 22, 832 (1980). Note the typographical errors in Table I.
[14] R. A. Brandenburg, Y. E. Kim, and A. Tubis, Phys. Rev. C 12, 1368 (1975).
[15] T. Sasakawa and T. Sawada, Phys. Rev. C 19, 2035 (1979).
[16] J. L. Friar, B. F. Gibson, and G. L. Payne, Z. Phys. A 302, (1981).
[17] J. L. Friar, B. F. Gibson, and G. L. Payne, Phys. Rev. C 22, 284 (1980).
[18] See Ref. 3, where this potential is used as a test case.
[19] R. A. Malfliet and J. A. Tjon, Nucl. Phys. A127, 161 (1969).
[20] H. P. Noyes, in *Three Body Problem in Nuclear and Particle Physics,* edited by J. S. McKee and P. M. Rolph (North-Holland, Amsterdam, 1970), p. 2.
[21] G. Eckart, Phys. Rev. 36, 878 (1930).
[22] J. K. L. MacDonald, Phys. Rev. 43, 830 (1933).
[23] G. Temple, Proc. Roy. Soc. London, Sect. A 119, 276 (1928).
[24] A. F. Stevenson and M. F. Crawford, Phys. Rev. 54, 375 (1938); A. F. Stevenson, *ibid.* 53, 199 (1938).
[25] D. H. Weinstein, Proc. Nat. Acad. Sci. (U.S.A.) 20, 529 (1934).
[26] R. L. Hall and H. R. Post., Proc. Phys. Soc. London 90, 381 (1967).
[27] R. N. Hill, J. Math. Phys. 18, 2316 (1977).

[28]F. Weinhold, Adv. Quantum Chem. 6, 299 (1972).
[29]L. M. Delves, J. Phys. A 5, 1123 (1972).
[30]E. W. Schmid and J. Schwager, Z. Phys. 210, 309 (1968).
[31]M. Walmsley, Proc. Phys. Soc. London 91, 785 (1967).
[32]E. W. Schmid, Y. C. Tang, and R. C. Herndon, Nucl. Phys. 42, 95 (1963).
[33]D. H. Bell and L. M. Delves, J. Comput. Phys. 3, 453 (1969); Nucl. Phys. A146, 497 (1970).
[34]I. R. Afnan and J. M. Read, Aust. J. Phys. 26, 449 (1973).